Eur. Phys. J. Appl. Phys. (2013) 64: 24504
DOI: 10.1051/epjap/2013120406

THE EUROPEAN PHYSICAL JOURNAL
APPLIED PHYSICS

Regular Article

Chaotic advection generated by Laplace forces in an electrolyte*

Gérard Vinsard[a], Stéphane Dufour, and Esteban Saatdjian

Université de Lorraine, LEMTA, UMR CNRS 7563, 54500 Vandœuvre-lès-Nancy, France

Received: 28 September 2012 / Received in final form: 14 December 2012 / Accepted: 28 January 2013
Published online: 8 November 2013 –

Abstract. Mixing and chaotic advection are studied in a liquid electrolyte set in motion by an electrical current passing through the fluid which is perpendicular to a magnetic field (Laplace force). Since the characteristic length in this system is very small, the inertia terms are negligible and the fluid motion is governed by the Stokes equations. Chaotic advection can occur in this flow if the potential between two electrodes is modulated time-periodically. Two tools have been implemented to characterize mixing in this flow. Poincaré sections are plotted in order to distinguish between regular and chaotic regions and the advection of a blob of dye injected into the liquid is calculated and successfully compared to experiments. This very small device is shown to be an effective fluid mixer.

1 Introduction

In certain medical and biological experiments it is necessary to mix a very small amount of a molecular substance into a similarly small amount of liquid solution. Molecular diffusion is a too slow process and agitation, if possible, is not an option because it would break the long molecules that are to be mixed. In these flows, at least one characteristic length is very small, between 10^{-3} and 10^{-6} m, the study of these particular flows is a relatively new science called *micro-fluidics.* Since the characteristic length is very small, the inertial forces in these flows are negligible and the motion is governed by the Stokes equations.

Chaotic advection (sometimes called Lagrangian turbulence) can be used to rapidly mix the long molecules into the fluid without breaking them. Chaotic advection is possible in two-dimensional time-dependent flows and in three-dimensional flows that are either spatially periodic or time-periodic. One apparatus that has been widely studied to study chaotic advection is the journal bearing flow [1], it consists of fluid between two eccentric rotating cylinders. When the two cylinders turn at constant velocity in opposite directions, a saddle point is formed in the region of minimum gap (homoclinic point). Perturbing this saddle point, for example by modulating the velocity of one cylinder time-periodically, leads to chaotic advection [2]. An interesting similar configuration but with two saddle points connected by two different streamlines (heteroclinic point) [3] showed that transport by chaotic advection was enhanced even further.

However, at the length scales considered here, moving boundaries or a system containing moving parts are not practical options. If the liquid is slightly conductive, as in most practical cases, an electrical current passing through the fluid and perpendicular to a magnetic field (Laplace force) can be used as the driving force to set the fluid in motion. Numerous flow configurations can be studied, finding the adequate geometry and position of each pair of electrodes and of the magnets is part of the problem. Chaotic advection can occur in a 2-D flow only if it depends on time. In the flows considered here this is relatively easy, one can just modulate the electrical current density of a given pair of electrodes.

The first aim of this work is to study a flow generated with only two magnets and an almost uniform current density, the coupling between electromagnetism and fluid mechanics is studied in detail. The electromagnetic generation of flows in an electrolyte can be used in many industrial applications, especially when the length scales are of the order of micro- or millimeters [4].

Setting fluids in motion as well as mixing different components in order to obtain a homogeneous mixture presents real difficulties at these small length dimensions. The flows generated by any driving force under these conditions are laminar, the trajectories of given particles of fluid are regular and do not lead to efficient mixing. Controllable body forces that can generate movement specifically adapted to mixing, i.e., rotational and time dependent (here time-periodic) so as to create chaotic advection, can overcome this drawback.

The second objective of this work is to describe and apply some models and tools that allow the analysis of electromagnetically induced mixing by chaotic advection. Chaotic mixing and its implementation by means of electromagnetic forces is a potential source of innovative future applications.

* Contribution to the Topical Issue "Numelec 2012", Edited by Adel Razek.

[a] e-mail: gerard.vinsard@ensem.inpl-nancy.fr

2 The MHD mixer and its modeling

The MHD mixer that we have designed consists of a tank (diameter 2.8 cm) containing the electrolyte (2 ml of copper sulfate solution with glycerol added to increase the viscosity, which has an electrical conductivity of 1.8 S/m) within which are disposed electrodes $\Gamma_{\rm s}$, $\Gamma_{\rm e}$, $\Gamma_{\rm n}$ and $\Gamma_{\rm w}$ (copper strips) for current injection using two voltage sources connected on one hand between $\Gamma_{\rm s}$ and $\Gamma_{\rm n}$ and on the other hand between $\Gamma_{\rm w}$ and $\Gamma_{\rm e}$. Two cubic magnets (5 mm, NdFeB, 0.5 T measured at their poles) are positioned below the tank as close as possible to the electrolyte. One magnet has its north pole and the other its south pole facing upwards.

This MHD mixer can effectively be built relatively easily, at least at the mm scale. Experiments are performed here to compare with numerical and analytical models.

2.1 Electromagnetic model

The steady-state electrical conducting model is sufficient to obtain the current density in the electrolyte, even if the electric field corresponding to the voltage supplied by the electrodes depends on time and even in the presence of a magnetic flux density due to the magnets and the current itself. In fact, the time variation is very small (the frequency is <1/10 Hz). On the other hand, the velocities in the electrolyte are also small (<10 mm/s) and the total current is <0.1 A.

With usual notation, D is the conductive region of the electrolyte, the electric scalar potential φ is a solution of the problem:

$$\begin{cases} \nabla \cdot \sigma \nabla \varphi = 0 \text{ in } D \\ \varphi = 0 \ \& \ V_n \quad \text{on } \Gamma_{\rm s} \ \& \ \Gamma_{\rm n} \\ \varphi = 0 \ \& \ V_e \quad \text{on } \Gamma_{\rm w} \ \& \ \Gamma_{\rm e} \\ \partial_n \varphi = 0 \qquad \text{on other boundaries} \end{cases}, \tag{1}$$

where σ is the conductivity of the electrolyte and V_n, V_e are the applied voltages. The boundaries Γ_x are defined in Figure 1. The current density $\boldsymbol{j}$ and Laplace force density $\boldsymbol{f}$ are, respectively:

$$\boldsymbol{j} = -\sigma \, \nabla \varphi \quad \text{and} \quad \boldsymbol{f} = \boldsymbol{j} \times \boldsymbol{b}, \tag{2}$$

where $\boldsymbol{b}$ is the magnetic flux density due to the magnets. A Coulombian description is used, the magnetic scalar potential is computed by an integral formulation, the sources are the magnetic charges on the north and south poles of the magnets (top and bottom faces of the cubes). Let us label $\Phi_e(z', \boldsymbol{x})$ (an intermediate variable that contains the geometric part of the magnetic scalar potential, which depends on $\boldsymbol{x} = x \ \boldsymbol{k}_x + y \ \boldsymbol{k}_y + z \ \boldsymbol{k}_z$ the point where the magnetic induction is needed and the vertical coordinate z' of a variable position inside the magnets $\boldsymbol{x}' = x' \ \boldsymbol{k}_x + y' \ \boldsymbol{k}_y + z' \ \boldsymbol{k}_z$) as

$$\Phi_e(z', \boldsymbol{x}) = \int_{-a/2}^{a/2} \mathrm{d}x' \int_{-a/2}^{a/2} \mathrm{d}y' \frac{1}{|\boldsymbol{x} - \boldsymbol{x}'|}. \tag{3}$$

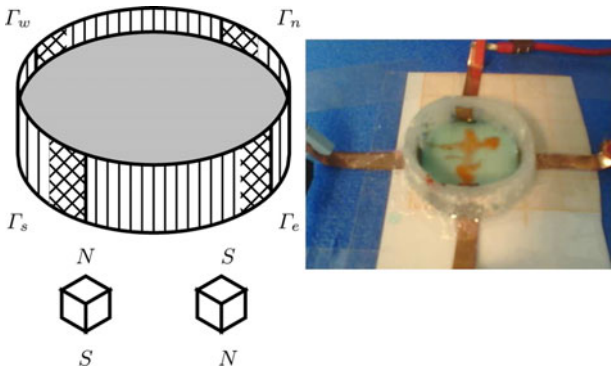

Fig. 1. Sketch of a circular disk containing the electrolytic solution, the positions of the electrodes and magnets (north and south poles are indicated approximately). The region D of the electrolyte is a cylinder whose boundary ∂D is split into $\Gamma_{\rm b}$, $\Gamma_{\rm t}$ (bottom and top), and $\Gamma_{\rm s}$, $\Gamma_{\rm e}$, $\Gamma_{\rm n}$, $\Gamma_{\rm w}$, its interface with the south, east, north and west electrodes. The other part of ∂D is not labeled. In the right figure is a photograph of the experimental setup.

If the two cubic magnets (of length a) are placed one beside the other below the circular tank, the magnetic flux density is

$$\begin{aligned} \frac{\boldsymbol{b}}{\mu_0 M} = {} & \nabla \Phi_e(0, \boldsymbol{x} + a/2 \boldsymbol{k}_x) - \nabla \Phi_e(0, \boldsymbol{x} - a/2 \boldsymbol{k}_x) \\ & - \nabla \Phi_e(-a, \boldsymbol{x} + a/2 \ \boldsymbol{k}_x) + \nabla \Phi_e(-a, \boldsymbol{x} - a/2 \ \boldsymbol{k}_x), \end{aligned} \tag{4}$$

where μ_0 is the vacuum permeability and M is the magnetic moment per unit volume of the magnets. The values of function Φ_e and its gradient are obtained by a closed analytical formula produced by a symbolic computation. The formula is too long to be written but it poses no singularity problems since the magnetic flux density is needed outside of the region enclosed by the north and south poles of the magnets.

As specified earlier, the voltages V_n and V_s depend on time but they vary very slowly (the typical period is 10 s) so that the transient state of the electromagnetic model is not necessary to be considered.

Even if the electrical problem (1) is in fact 2-D and, in order to simplify the connection with the fluid flow computations, which is 3D as explained below, the scalar potential is computed with the finite element method in a 3-D tetrahedral mesh with a P2 interpolation. The magnetic field is obtained by an approximation of the magnetic induction values on this P2 basis and then the Laplace force density, which is used verbatim on the same mesh as for the fluid flow computation, becomes piecewise P1 in each element.

2.2 Flow field calculation

As stated earlier, the velocities in the electrolyte are sufficiently small so that inertial effects can be neglected. The flow field is calculated by solving the Stokes equations over

the entire domain. For velocities in the range of 1 mm/s, a characteristic length dimension of $L = 5$ mm corresponding to the size of magnets and a kinematic viscosity of 10^{-5} m^2/s the value of the Reynolds number $\rho/\mu\ L\ v$ is 0.5. Furthermore, the flow is assumed to be at steady state at each time instant (quasi-static approximation). The period used for the time dependence of the voltages is $T \approx 10$ s so that the corresponding Strouhal number $L/(T\ v)$ is 0.5. This confirms our hypothesis, comparison with experiments later on will also justify this.

The velocity field $\boldsymbol{v}$ is then computed by solving the creeping-flow equations [5]:

$$\left.\begin{array}{l}\mu\nabla\times\nabla\times\boldsymbol{v}+\nabla P=\boldsymbol{f}-\rho\ g\ \boldsymbol{k}_z\\ \nabla\cdot\boldsymbol{v}=0\end{array}\right\}\text{in } D, \tag{5}$$

where $\mu \approx 10^{-2}$ Pa s is the fluid viscosity, $\rho \approx 10^3$ m^3/s is the fluid density, g is the gravitational acceleration and P is the pressure. The driving force $\boldsymbol{f}$ is the Laplace force density $\boldsymbol{f}$. It is time dependent because the voltages V_n and V_e are time dependent. Thus the velocity field is also time dependent.

The boundary ∂D of the electrolyte has two components: Γ_t the top interface (free surface) and $\partial D_t = \partial D/\Gamma_\mathrm{t}$ the complementary boundary. The normal component of the velocity vanishes everywhere on this boundary

$$\boldsymbol{v}\cdot\boldsymbol{n}=0\ \text{ on }\ \partial D. \tag{6}$$

There is also the no-slip condition on ∂D_t

$$\boldsymbol{v}\times\boldsymbol{n}=\boldsymbol{0}\ \text{ on }\ \partial D_t. \tag{7}$$

If $\overline{\overline{D}}$ is the rate-of-strain tensor and P_0 is the atmospheric pressure then, neglecting the shear stress at the free surface, the force balance at the free surface Γ_t is

$$-P\boldsymbol{n}+2\mu\overline{\overline{D}}\boldsymbol{n}=-P_0\boldsymbol{n}\ \text{ on }\ \Gamma_\mathrm{t}. \tag{8}$$

This is a free boundary problem, the shape of the free surface Γ_t has to be computed [6]. To simplify the calculations and since the velocities are small, it is possible to assume that Γ_t is flat. Then if the velocity is

$$\boldsymbol{v}=u\boldsymbol{k}_x+v\boldsymbol{k}_y+w\boldsymbol{k}_z, \tag{9}$$

the tangential part of (8) combined with (7) ($w = 0$ on Γ_t) becomes

$$\partial_n u=\partial_n v=0\ \text{ on }\ \Gamma_\mathrm{t}, \tag{10}$$

and can be completed with (6) applied to the normal component w of $\boldsymbol{v}$ on Γ_t as

$$w=0\ \text{ on }\ \Gamma_\mathrm{t}. \tag{11}$$

The computation model of the fluid flow is still established in 3-D: (5) in the electrolyte region D, (6) and (7) on ∂D_t and (10), (11) on Γ_t. The region D has a small thickness in the $\boldsymbol{k}_z$ direction and the components u and v are larger than w. However the 3-D model is still needed to take into account both the viscous friction with the bottom of the tank and the 3-D nature of the electromagnetic force density.

The Stokes equations lead to a saddle point problem since pressure is in fact a Lagrange multiplier of the zero divergence constraint on the velocity. The Uzawa algorithm [7] (the pressure being given, the velocity is computed without taking into account the zero divergence constraint; when the velocity is given, the pressure distribution is computed by using the previously obtained divergence; calculations are resumed until convergence is attained) is used with the help of a P2 interpolation on each tetrahedron for the velocity components and P1 for the pressure field.

2.3 Advection model

The Eulerian velocity field has been calculated above. However, to implement several tools useful in the study of chaotic advection, the trajectories of fluid particles in the flow (Lagrangian tracking) are necessary. The trajectories of liquid particles in the flow may be computed by solving:

$$X(t)\in D \text{ such as } \left\{\begin{array}{l}\frac{\mathrm{d}\boldsymbol{k}}{\mathrm{d}t}=\boldsymbol{v}(t,\boldsymbol{X})\\ \boldsymbol{X}(0)=\boldsymbol{x}_0\end{array}\right.\in D\ , \tag{12}$$

where $\boldsymbol{x}_0$ is the initial fluid particle position.

As stated above, due to the very small depth of the electrolyte, the w component of the velocity field (9) is also small and the liquid particles are almost only advected in the $\boldsymbol{k}_x, \boldsymbol{k}_y$ plane. If the trajectories are assumed to lie only in this plane, then (12) reduce to the following 2-D problem:

$$X(t)\in \Gamma_\mathrm{t} \text{ such as } \left\{\begin{array}{l}\frac{\mathrm{d}\boldsymbol{X}}{\mathrm{d}t}=\boldsymbol{v}_t(t,\boldsymbol{X})\\ \boldsymbol{X}(0)=\boldsymbol{x}_0\end{array}\right.\in \Gamma_\mathrm{t}\ , \tag{13}$$

where

$$\boldsymbol{v}_t=u(z=e)\ \boldsymbol{k}_x+v(z=e)\ \boldsymbol{k}_y. \tag{14}$$

Two tools can be used to estimate the degree of mixing in this flow [8]. The first one is the Poincaré section; the trajectories of several initial positions, identified by different colors, are calculated and the position at the end of each period of the given time-periodic protocol is plotted. After many periods (say 1000), the Poincaré section will show qualitatively regions where there is mixing and regions where there is no mixing. The Poincaré sections plotted here use the assumption that the flow is two-dimensional, they give an indication of the long-term mixing behavior of this flow.

The second tool is dye advection experiments; a blob of dye, composed of a certain number of particles and at a given initial position, is advected by the velocity field. The shape of the blob during the process and the length of the blob at the end of each period indicate, qualitatively, the short-term mixing behavior is studied with this tool. These numerical experiments can be compared to real experiments to test the several assumptions regarding the flow used above.

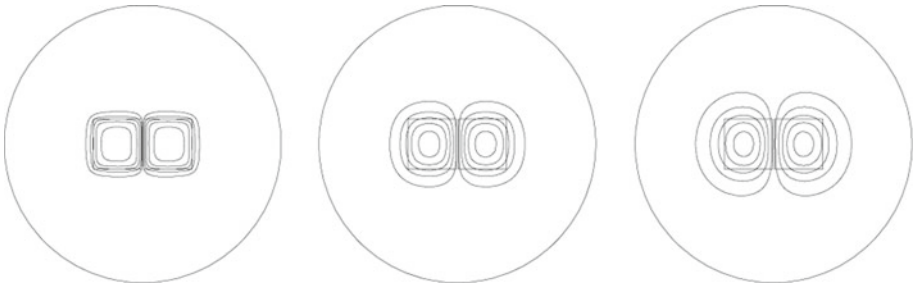

Fig. 2. The $\boldsymbol{k}_z$ component of the magnetic flux density for $z = 0$ (bottom), 1 mm and 2 mm (top of the electrolyte).

The velocity field in the 2-D triangular finite element mesh of the boundary Γ_t inherits the P2 approximation on the 3D mesh. However to simplify the calculations, the approximation is weakened to P1 for the Poincaré sections and the dye advection experiments. Then the integration of (12) can be performed exactly in each element and the algorithm consists in the tracking of the next element to start again the integration process. The obtained times and positions are connected to each other, it is sufficient to plot the Poincaré sections.

The dye advection experiment requires a supplementary task. The blob is represented as a connected set of points on a broken closed line and after that each of these points is advected, this connection can become too coarse. The distance between two adjacent points which are the extremities of a linear segment becomes too large (if there is chaotic advection), then the segment is broken into two segments built with the middle point and the process of advection is repeated with these two segments (preserving the results already obtained). The algorithm is implemented in a recursive way.

Both methods are qualitative although one can quantify the stretching and mixing by calculating the length of the blob. The optimum modulation frequency was determined empirically; in a future study we will use the Melnikov method [2,8] to obtain a more rigorous result.

3 Results

3.1 Electromagnetic fields and fluid flow

Figure 2 shows the $\boldsymbol{k}_z$ component of the magnetic flux density (4), which is important in the expression of the Laplace force density (2). This component varies strongly with the distance to the magnets, this dependence cannot be neglected.

Figure 3 shows the streamlines corresponding to the 2-D velocity field (14). They are computed from $\boldsymbol{v}_u$ by minimizing the functional

$$\psi \longrightarrow \int_\Gamma (u\boldsymbol{k}_x + v\boldsymbol{k}_y - \nabla\psi \times \boldsymbol{k}_z)^2 \mathrm{d}x\mathrm{d}y, \qquad (15)$$

with respect to any ψ which vanishes on the boundary of Γ_t. The minimizing argument is also denoted ψ and its iso-values are the streamlines.

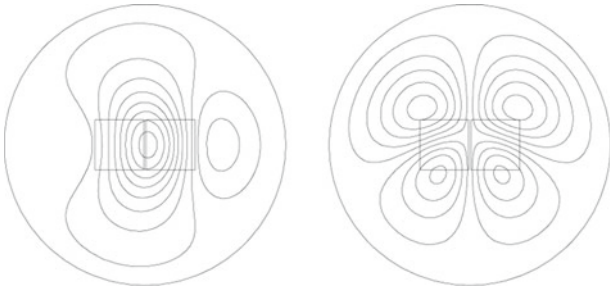

Fig. 3. Streamlines of the 2-D velocity field $\boldsymbol{v}_u$ on Γ_t for the configurations where the current lines are (almost) horizontal (left) and vertical (right).

These streamlines are computed for the two orthogonal configurations where only one of the four electrodes has a unity potential and the others are connected to the ground: on the left the east electrode and on the right the north one. The flows patterns are dominated: on the left by an elliptic point (except for the small recirculation on the right) and on the right by a hyperbolic saddle point.

3.2 Advection

If only one of the preceding velocity fields is used any point is advected along its streamline then there is no mixing by chaotic advection. The shape of a blob of dye changes but inside a bounded region (the region bounded by the two streamlines where the blob was placed initially). If the two configurations are used time-periodically:

$$\underset{\text{(elliptic flow)}}{V_e = V\ \sin(2\pi\ f\ t)};\ \underset{\text{(hyperbolic flow)}}{V_n = V(1 + \cos(2\pi\ f\ t))}, \qquad (16)$$

then the global flow becomes unsteady and also chaotic mixing occurs.

The goal here is to find values of the parameters V and ω that can generate complex trajectories for a given particle, which ideally go everywhere inside Γ_t. We have used a voltage $V = 1$ V and a frequency $f = 0.05$ Hz. An initial blob is introduced at the center of the electrolyte; its surface is $\approx$25 mm^2 and its perimeter is $\approx$12 mm. The shape of the blob is photographed at the end of each period during the experiment. A computation using the described model is also performed and a comparison is shown Figure 4 for a sequence of nine periods.

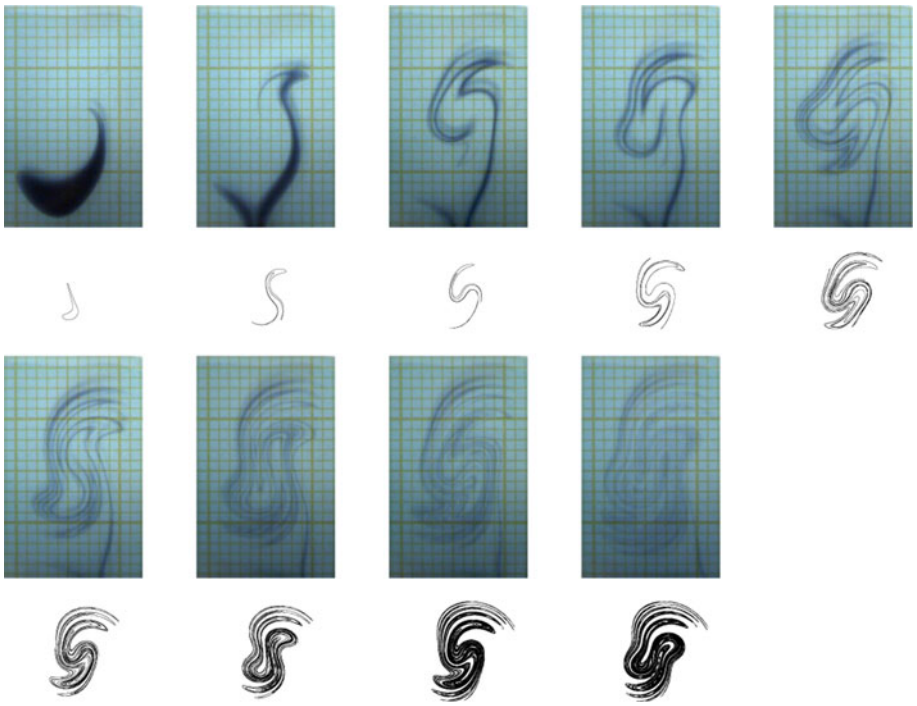

Fig. 4. Sequence of blob of dye shape at times $0, 1/f, \ldots 9/f$. Experiment (up) and computation (down).

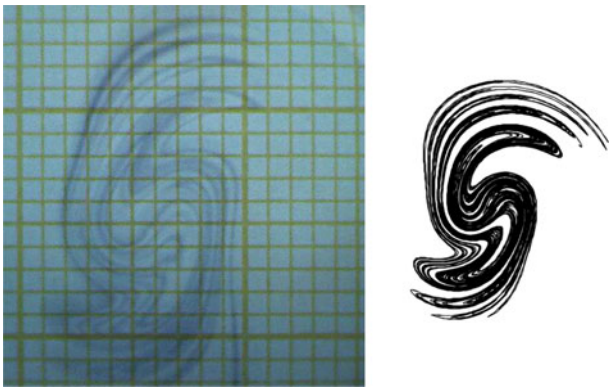

Fig. 5. Zoom of the blob at $8/f = 160$ s.

Although the shapes of the blobs are not exactly the same (due to the uncertainty in the initial location of the blob), the qualitative agreement is very good. Figure 5 shows a zoom at the end of period 8. One can note from the figure that the experiments and the numerical code give the same number of striations, the stretching and folding characteristic of chaotic advection. One can conclude that numerical computations and experiments are in good agreement, thus validating the several hypotheses given above.

The dye advection experiments can only be performed for a limited amount of periods because the stretching and folding of the blob leads to a dramatic increase in the number of points needed to describe its boundary and in the total amount of computations of ODE (13).

In Figure 6 we plot the perimeter of the blob versus time. The initial length is 12 mm, the plot shows that it increases exponentially and reaches a length of 10 m in

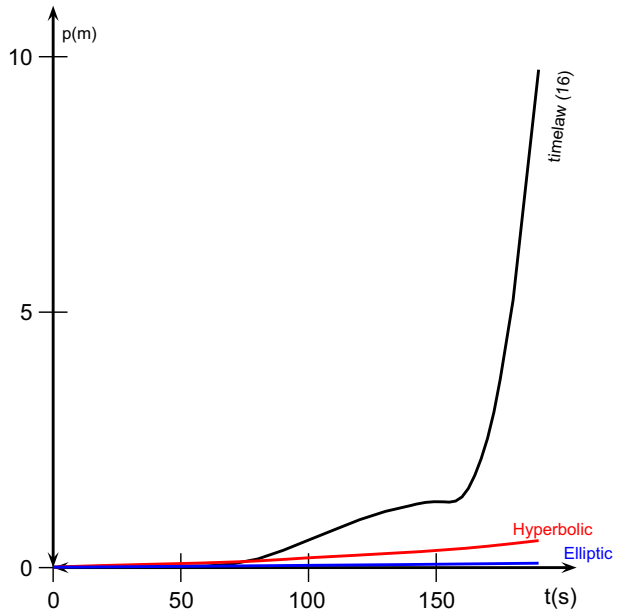

Fig. 6. Perimeter of the blob versus the time. The curves labeled hyperbolic and elliptic corresponds to the computation in these cases.

8 periods. We also estimate the average thickness of the blob, it is 25 mm^2/10 m ≈ 2.4 μm at the end of 8 periods. This small thickness, for which transfer by diffusion is important, explains why the details of the blob disappear in the experiment even with a zoom.

The Poincaré section method allows to analyze the long-time advection process. Figure 7 shows the 8 initial points, the 8×11 points corresponding to the position of

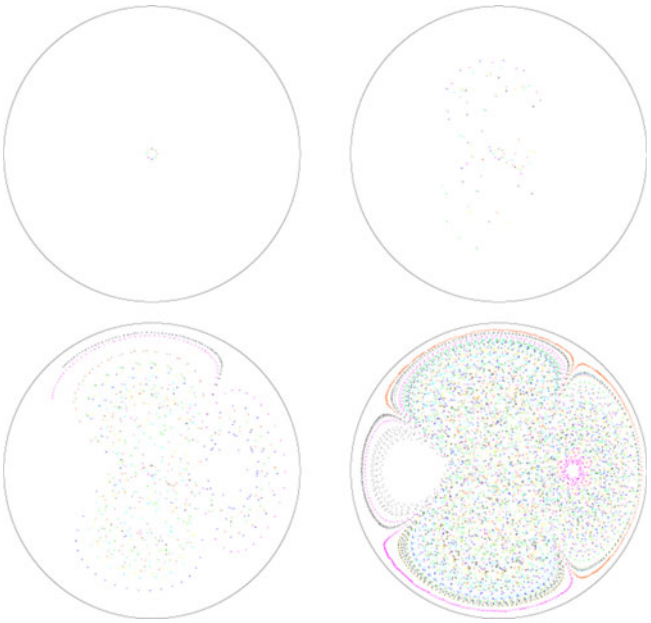

Fig. 7. Poincaré sections for 0, 10, 100, and 1000 periods.

these initial points at the end of each period (10 periods), 100 periods and, finally, 1000 periods.

At the end of 1000 periods, the Poincaré section shows that chaotic advection occurs practically everywhere except near the outer surface and in a regular island on the left part of the figure. The region of mixing has the shape of a quadripole which is the image of the used forcing based on the rotation of the hyperbolic flow pattern.

4 Conclusion

Chaotic mixing of fluids in very small devices, an important engineering problem today, can be obtained by using a time-periodic Laplace force to set the fluid in motion. The apparatus presented here consists of a liquid electrolyte in a circular container, two sets of electrodes and two magnets placed in the bottom are responsible for the Laplace force. The flow equations have been solved for the non-inertial case and dye advection numerical experiments have been compared successfully to real experiments. Poincaré sections have also been plotted. The length of this device can be reduced by an order of magnitude in the future. Future work will deal with improving the modulation protocol. Here, the electrical supply is the superposition of a DC current and a two-phase AC current, a three-phase current could probably give improved results.

References

1. P.D. Swanson, J.M. Ottino, J. Fluid Mech. **2130**, 227 (1990)
2. J.M. Ottino, *The Kinematics of Mixing: Stretching, Chaos, and Transport* (Cambridge University Press, UK, 1989)
3. E. Saatdjian et al., Phys. Fluids **8**, 677 (1996)
4. S. Qian, J. Zhu, H.H. Bau, Phys. Fluids **14**, 3584 (2002)
5. G. Leal, *Advanced Transport Phenomena: Fluid Mechanics and Convective Transport Processes* (Cambridge University Press, UK, 2010)
6. G. Vinsard, S. Dufour, J.-P. Brancher, IEEE Trans. Magn. **45**, 1562 (2009)
7. R. Glowinski, O. Pironneau, in *Numerical Methods for the Stokes Problem. Chapter 13 of Energy Methods in Finite Element Analysis*, edited by R. Glowinski, E.Y. Rodin, O.C. Zienkiewicz (J. Wiley & Sons, Chichester, UK, 1979), pp. 243–264
8. S. Sadhan, G. Metcalfe, J.M. Ottino, J. Fluid Mech. **269**, 199 (1994)